Supplementary Information

Fabrication of Zinc-Dicarboxylate- and Zinc-Pyrazolate-Carboxylate-Framework Thin Films through Vapour-Solid Deposition

Raghavender Medishetty,[a],* Zongji Zhang,[a] Alexander Sadlo,[a] Stefan Cwik,[a] Daniel Peeters,[a] Sebastian Henke,[b] Nagarathinam Mangayarkarasi,[c] Anjana Devi[a],*

[a] Chair of Inorganic Chemistry II, Inorganic Materials Chemistry, Ruhr-Universität Bochum, Universitätsstraße 150, 44801 Bochum, Germany.

[b] Inorganic Chemistry, Faculty of Chemistry and Chemical Biology, Technische Universität Dortmund, Otto-Hahn-Straße 6, 44227 Dortmund, Germany.

[c] Department of Chemistry, National University of Singapore, Science Drive 3, 117543 Singapore.

1. General details

All the chemicals were purchased of reagent grade and used without further purification. The X-Ray diffraction (XRD) measurements were performed using a Bruker AXS D8 Advance instrument, (Bragg–Brentano, measurement range: $2\theta = 3–50°$) using Cu Kα radiation (1.5418 Å). Thermogravimetric analyses (TGA) of the powdered **1** were collected using a TG/DSC NETZSCH STA 409 PC instrument under N_2 (99.999%) gas flow (300 ml·min^{-1}) and the TGA of H_2bdc was analysed using Seiko TG/DTA 6200/SII at ambient pressure (sample mass ≈ 10 mg, N_2 flow rate = 300 mL min^{-1}), with a heating rate of 5 °C min^{-1} from the temperature range of 30–600 °C. Elemental Analyses (EA) were performed at the department of Analytical Chemistry, Ruhr-University Bochum. UV-Vis spectroscopy was performed at room temperature on an Agilent Cary 5000 double beam spectrophotometer, using transparent fused silica substrates. Single crystal X-ray diffraction data were collected on an Agilent Technologies SuperNova diffractometer with an Atlas CCD detector and Cu Kα radiation from a microfocus X-ray source with multilayer X-ray optics. The scanning electron microscopy (SEM) images were recorded from an FEI ESEM Dual Beam™ Quanta 3D FEG microscope.

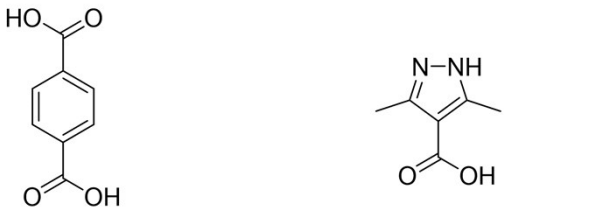

1,4-benzenedicarboxylic acid (H_2bdc) 3,5-dimethyl-4-carboxypyrazole (H_2dmcapz)

Figure S1 | Molecular structures of H_2bdc and H_2dmcapz.

2. Syntheses of thin films and MOFs

Preparation of ZnO CVD thin films:
ZnO thin films were deposited on 2 x 3 cm² Si(100) (Siegert Consulting) in a custom built, horizontal cold-wall, low pressure CVD reactor using a modified procedure reported by Bekermann *et al*.[1] The substrates were cleaned prior to film deposition by a sequence of rinsing with 2-propanol and 10 minutes sonication in water in order to remove surface contaminations. The [Zn(mpki)$_2$] precursor was vapourized at 120 °C and delivered to the substrate by a nitrogen gas flow (50 sccm). Standard conditions during CVD experiments were set to a pressure of 1 mbar, duration of 30 minutes per deposition, an oxygen gas flow of 50 sccm and a substrate temperature of 600 °C. The thickness of these films was determined by using Filmetrics F30 system (it was measured at six different positions on the wafer to confirm the uniformity and thickness of the film) and along with SEM measurements (Figure S13 and S14).

Annealing of ZnO thin films: The as-prepared ZnO thin films were annealed in a heating chamber at 700 °C for 2h at atmospheric conditions.

UV-Vis absorption measurements: ZnO thin films have been grown on quartz slides and then these films were converted into MOF as described above and used for UV-Vis absorption measurements.

Method-1: (Quartz tube chemical vapour reaction + closed cell treatment)

Quartz tube chemical vapour reaction: ZnO thin films (1 x 1.5 cm^2) were mounted on a custom-built reactor as shown in Figure S2 and the crucible in the thermostat has been loaded with 100 mg of linker. A carrier gas flow (Ar) of 200 ml/min was bubbled through respective solvent (AcOH/DMF with 1:1 (v/v) ratio in the case of **1** and water in the case of **2**), followed by heating the thermostat (at 240 °C for 3 h in the case of **1** and at 170 °C for 3 h in the case of **2**) at ambient pressure. After the reaction, the substrate was cooled, characterized by XRD and then used for closed cell treatment.

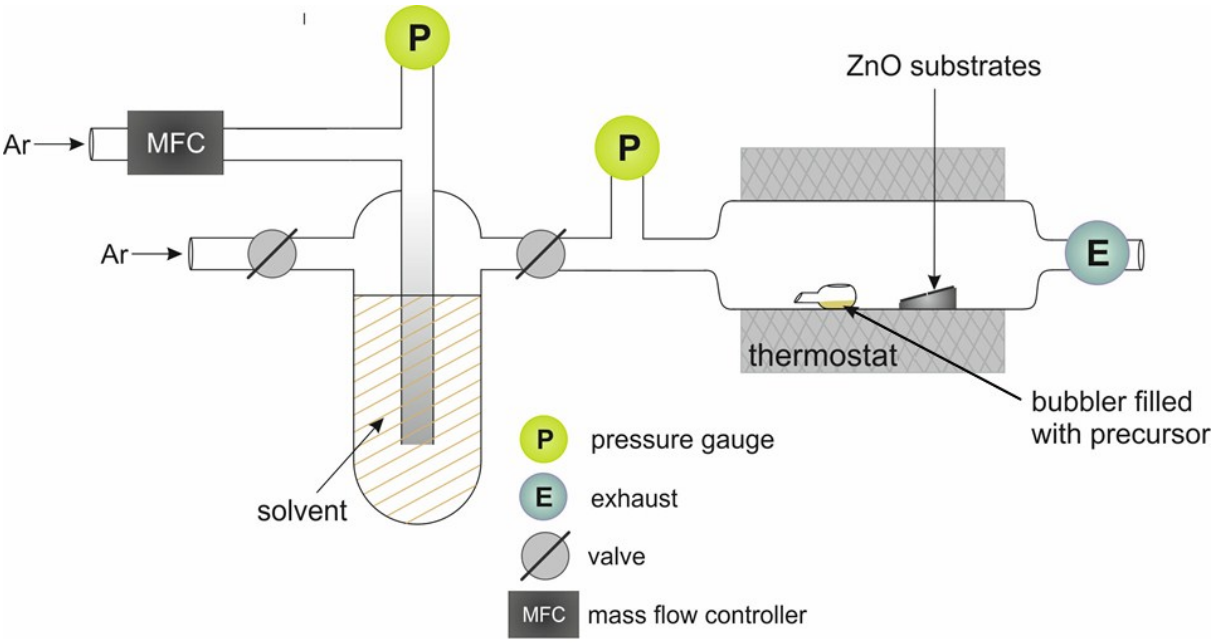

Figure S2 | Schematic view of the custom-built quartz tube chemical vapour reactor to convert metal-oxide thin films into composites.

Closed cell treatment: After analysis of the above mentioned composite thin films, the substrates have been placed inside a closed chamber either without solvent or 100 µL methanol at the bottom of closed reactor, then this reactor was placed in an oven at 120 °C for 24 h and then the substrates have been used for XRD and electron microscopy analyses.

Method-2

ZnO thin films (1.5 x 1.5 cm^2) were placed above the 5 ml vials which contain 100 mg of H_2dmcapz as shown below. This set-up has been heated at 170 °C for 48 h in hot air oven.

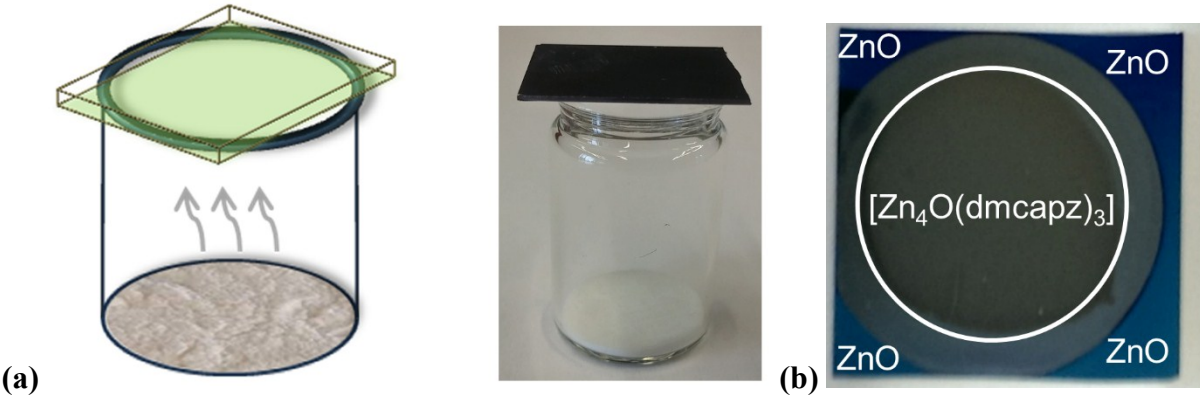

Figure S3 | (a) Schematic view showing the reaction of ZnO film with H_2dmcapz vapours. **(b)** ZnO substrate after the reaction, the central part of the ZnO film has been converted into **2** and the unreacted (unexposed, blue part) area was shown with ZnO. This is outside the glass vial with no, or limited exposure of H_2dmcapz vapours.

3. Thermogravimetric analyses (TGA)

TGA of H_2bdc: H_2bdc is one of the most used organic linkers in the field of MOFs and coordination polymers. Hence, this linker has been chosen for the synthesis of MOF thin films through vapour phase procedures. TGA of H_2bdc has been performed (Figure S4) to understand the evaporation procedures, which reveals a one-step weight loss between 250 – 350 °C with a residual mass close to 0%, indicative of a clean evaporation process. Based on the TGA, the stability of the compound under processing conditions was investigated via isothermal TG at 240 °C (Figure S5), which shows a linear weight loss over 3 h at 240 °C, demonstrating a constant mass supply/transport during the whole CVD process with a rate of 14.5 µg/min.

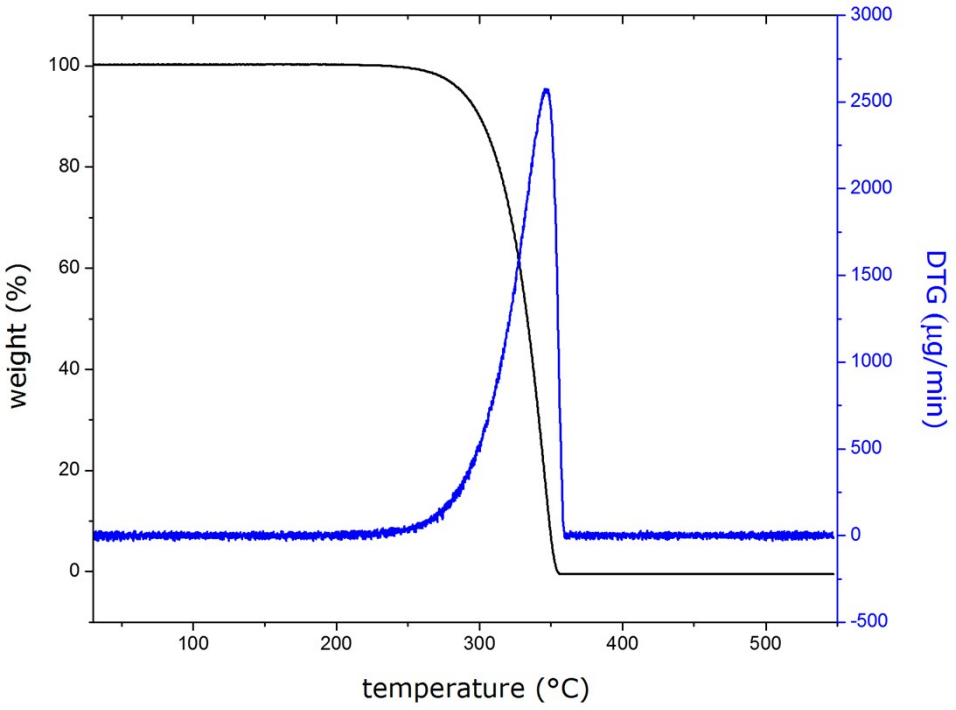

Figure S4 | TGA (black trace), DTG (blue trace) curves of H_2bdc with a heating rate of 5 °C·min^{-1} under N_2 flow of 300 ml·min^{-1}.

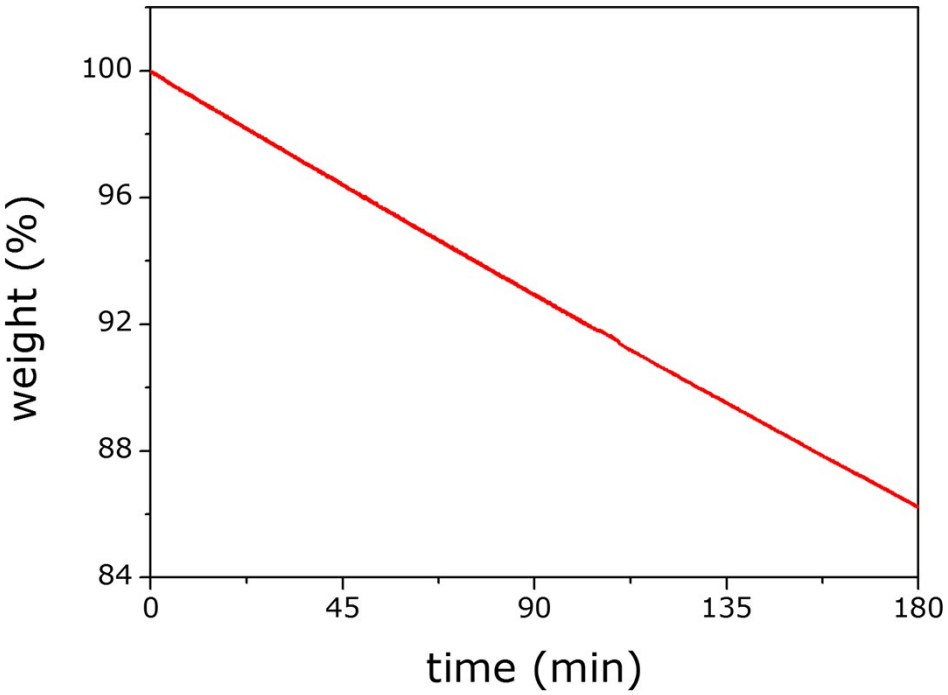

Figure S5 | Isothermal TG analysis of H_2bdc at 240 °C under N_2 flow of 300 ml·min^{-1}.

TGA of H_2dmcapz: H_2dmcapz (combination of O and N coordination) has been chosen for the synthesis of MOF thin films thorough vapour phase procedures. TGA showed a one-step weight loss between 180 – 260 °C with a residual mass close to 0%.

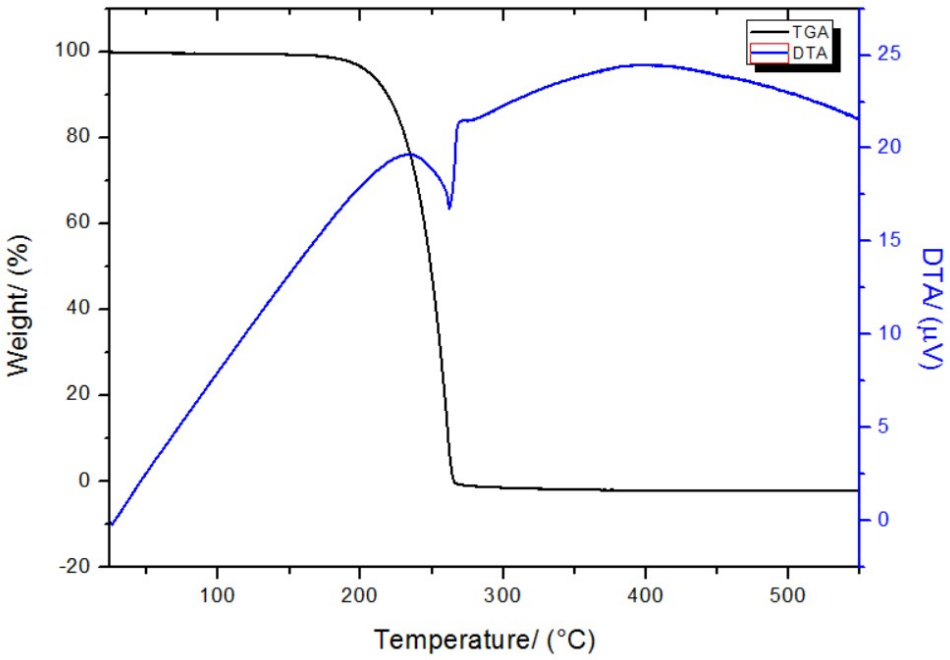

Figure S6 | TGA (black trace) and DTA (blue trace) curves of H_2dmcapz with a heating rate of 5 °C·min^{-1} under an N_2 flow of 300 ml·min^{-1}.

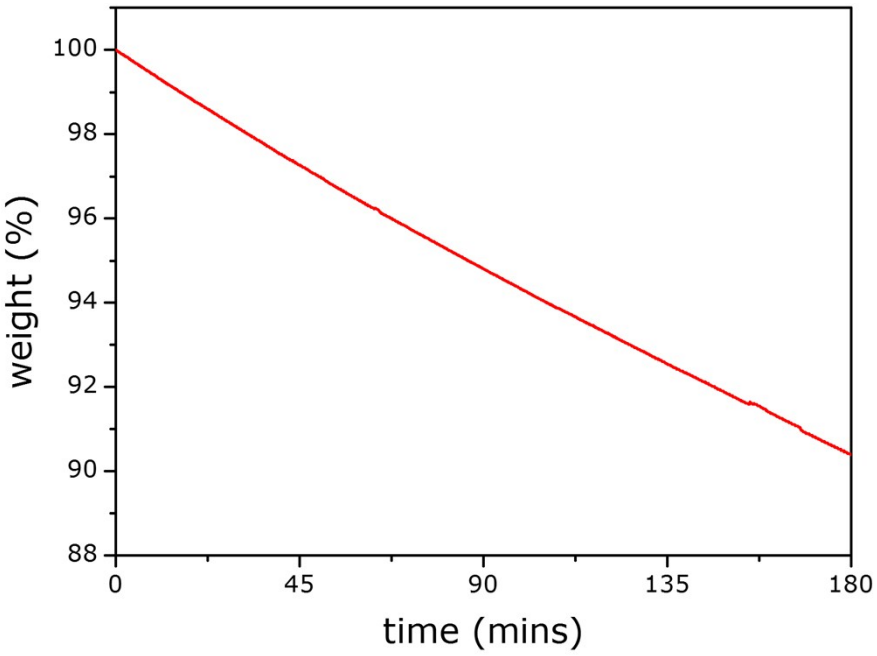

Figure S7 | Isothermal TG analysis of H_2dmcapz at 170 °C under N_2 flow of 300 ml·min^{-1}.

4. X-ray diffraction (XRD) analyses

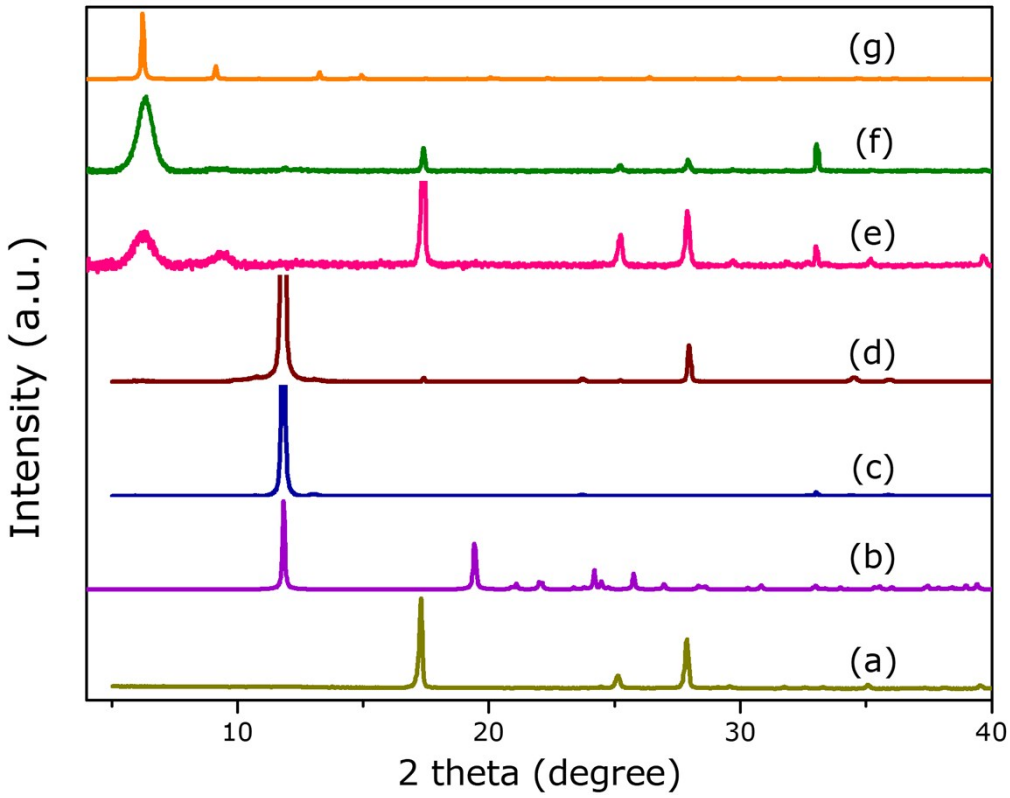

Figure S9 | XRD patterns of the **(a)** commercially available H_2bdc powder, **(b)** simulated XRD pattern of monoclinic anhydrous $Zn(OAc)_2$,[2] **(c)** ZnO substrates treated with AcOH/DMF at 240 °C for 3 h and the formation of [200] preferred oriented anhydrous $Zn(OAc)_2$, **(d)** ZnO substrates treated with H_2bdc in the presence of AcOH/DMF at 240 °C for 3 h, **(e)** ZnO substrate treated with H_2bdc in the presence of AcOH/DMF at 240 °C for 15 h, **(f)** annealed ZnO (700 °C for 2 h) substrate treated with H_2bdc in the presence of AcOH/DMF at 240 °C for 15 h and **(g)** calculated XRD pattern of MOF-5.[3]

The AcOH and DMF have been chosen for the preparation of **3**, because AcOH is expected to convert the less reactive ZnO film into more reactive $Zn(OAc)_2$ as an intermediate.[2] During this, a highly crystalline and monoclinic $Zn(OAc)_2$ thin film has been observed (Figure S9). Similarly, DMF has been chosen which would be helpful for the reactivity of dicarboxylic acid and the formation of MOF thin film. Attempts have been made by using various other solvents and their combinations, however, most of these deposition experiments did not yield any positive results so far.

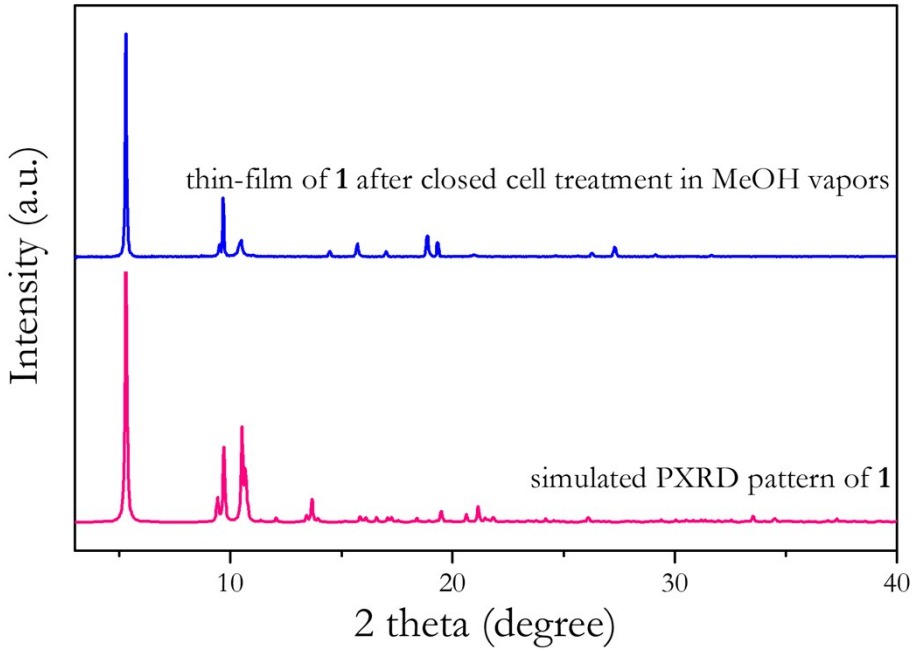

Figure S10 | Experimental XRD pattern of a thin film of **1** in comparison to the diffraction pattern simulated on the basis of its single crystal structure.

5. Scanning electron microscopy (SEM) analysis

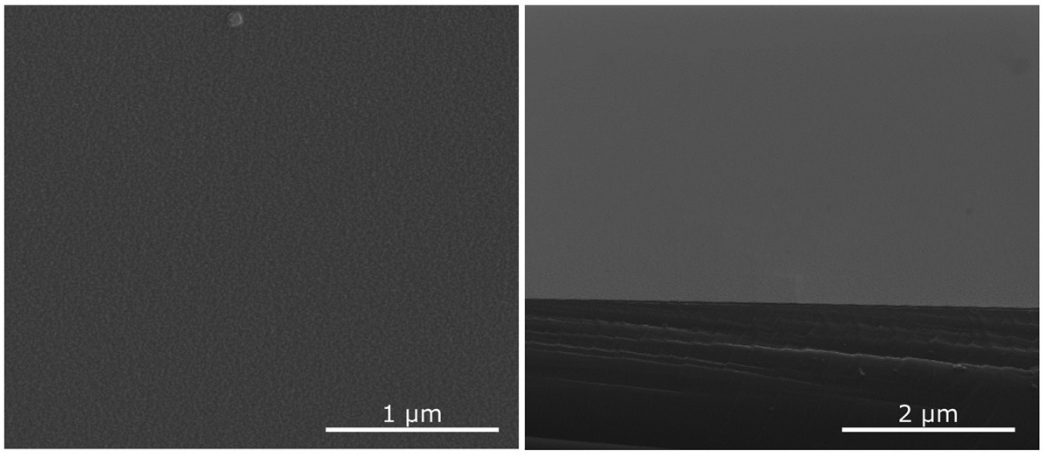

Figure S11 | SEM images of as-synthesized ZnO substrates at 600 °C.

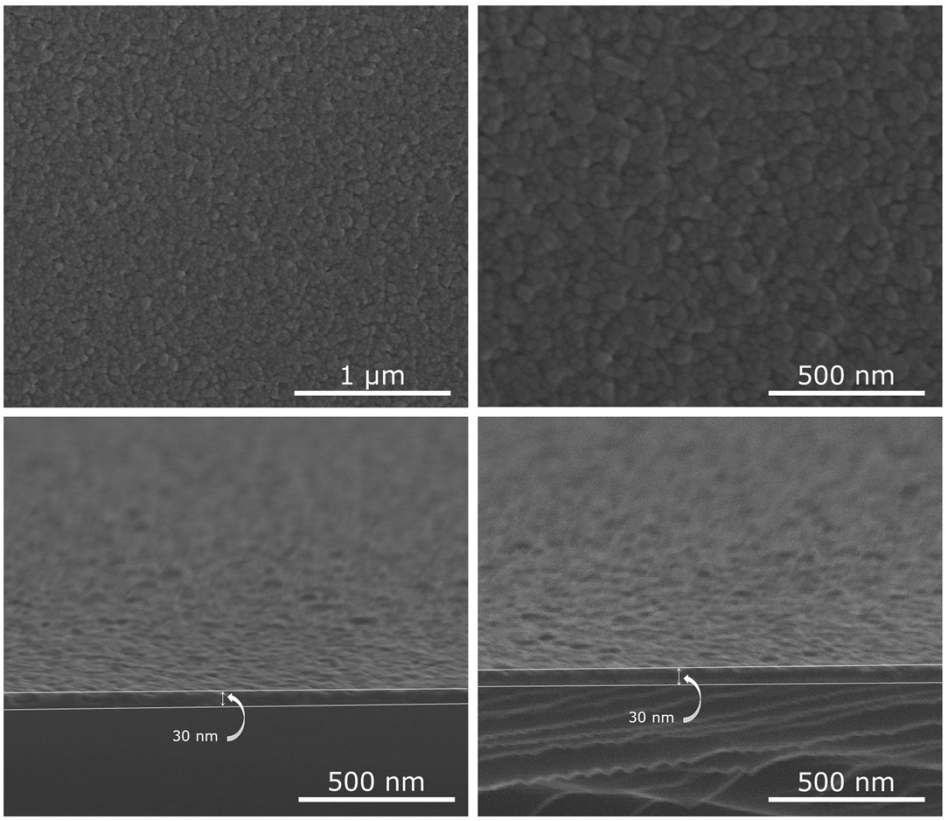

Figure S12 | SEM images of ZnO substrates after annealing at 700 °C for 2 h.

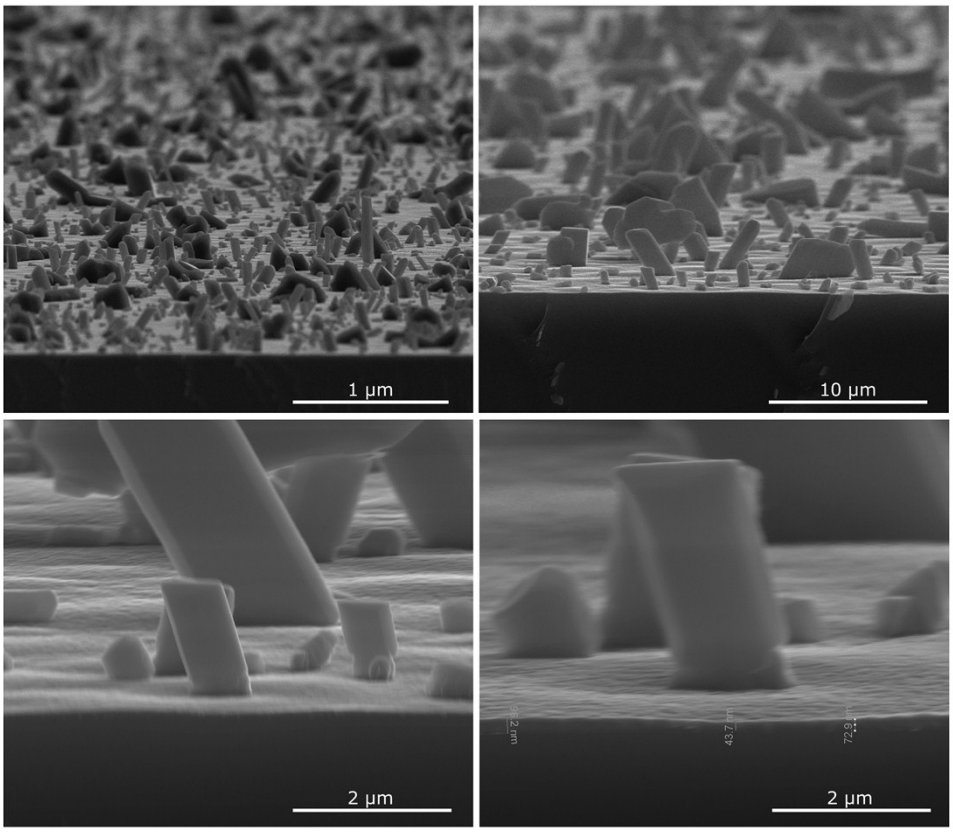

Figure S13 | SEM images of composite **3** (side view).

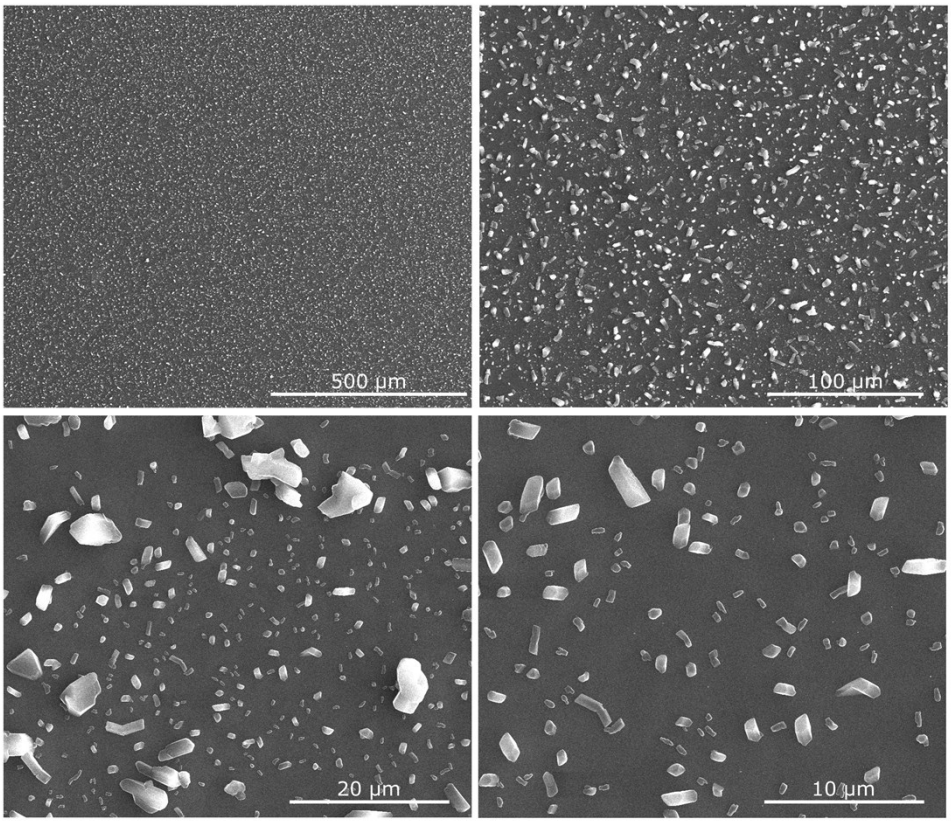

Figure S14 | SEM images of composite **3** (top view).

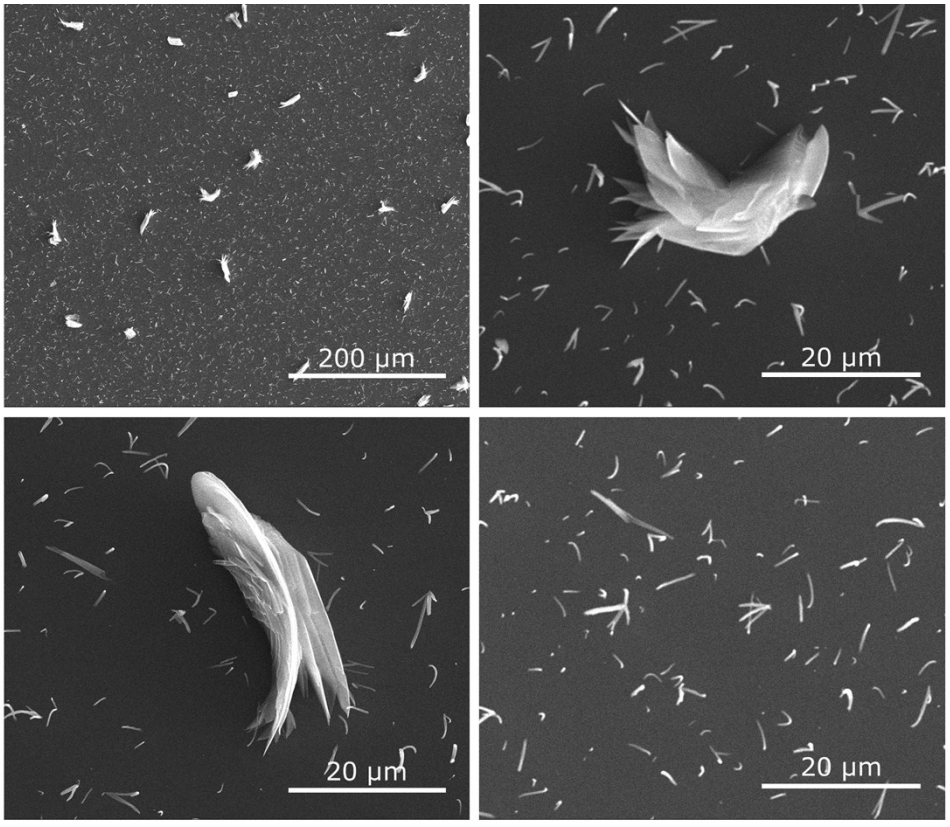

Figure S15 | SEM images of ZnO substrate after the CVD tube reaction with H_2dmcapz.

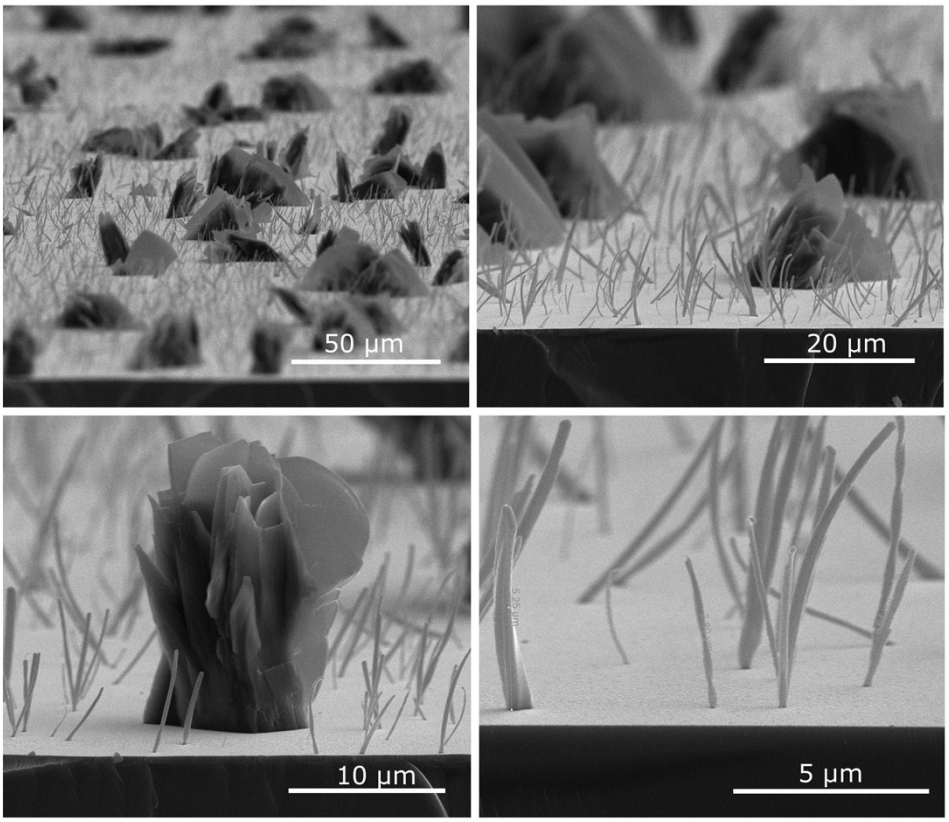

Figure S16 | SEM side view images of ZnO substrate after the CVD tube reaction with H_2dmcapz.

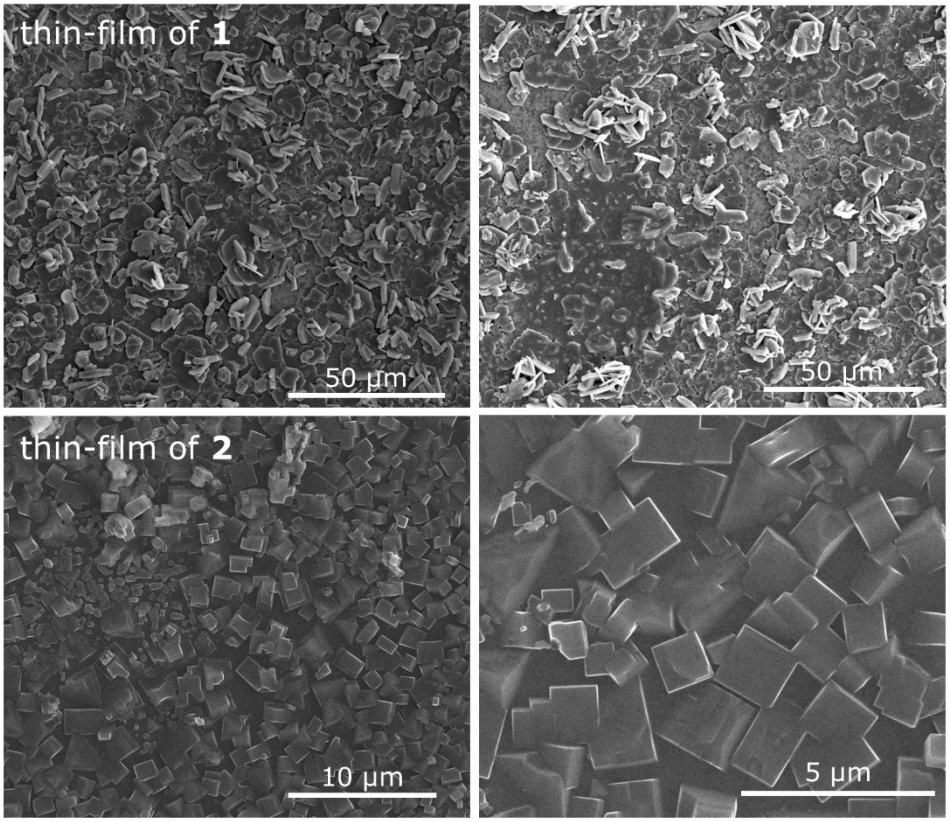

Figure S17 | SEM top view images showing the uniform coverage of the MOF crystallites of **1** (top) and **2** (bottom) on Si-substrate. Dominance of crystallites of **2** along [200] direction.

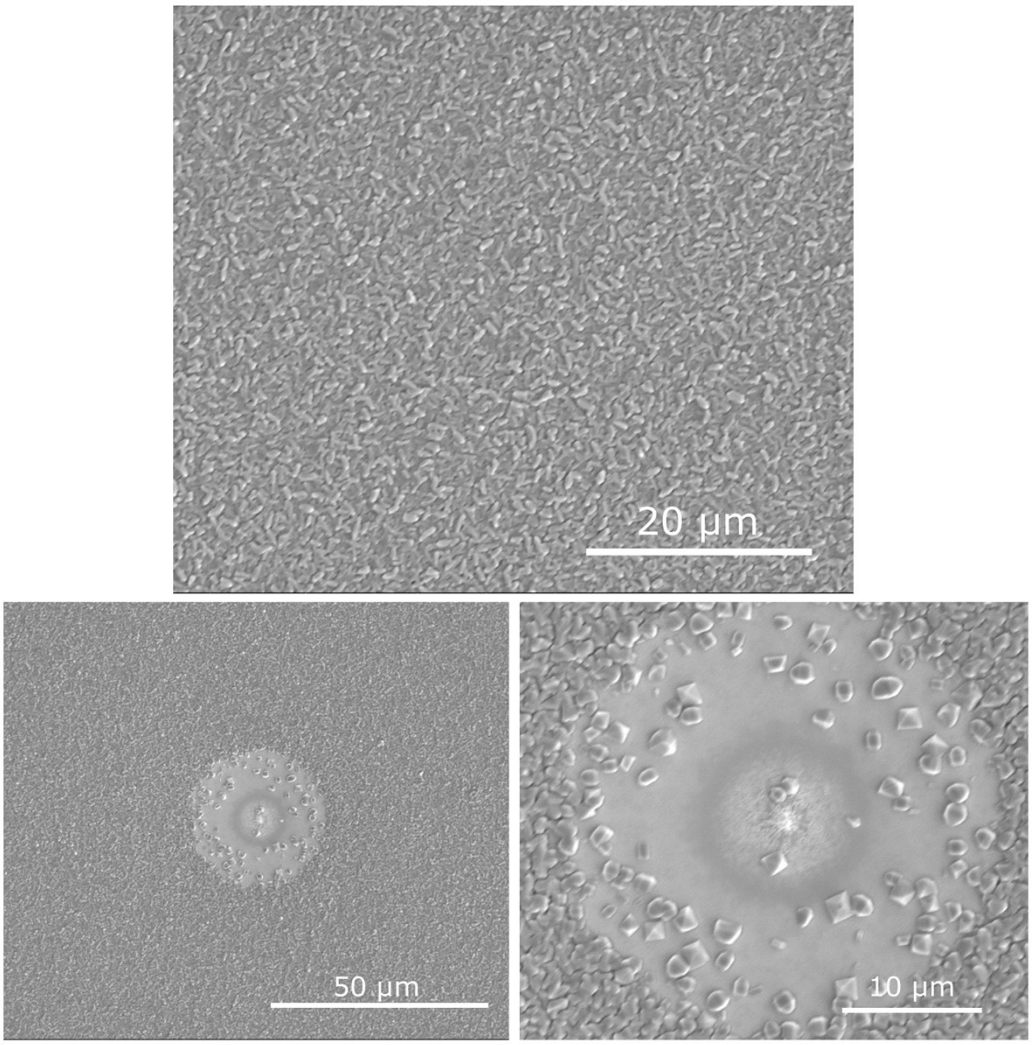

Figure S18 | SEM micrographs of MOF film after the reactivity of ZnO thin film with H_2dmcapz vapours. Top image shows the complete and uniform distribution of MOF crystallites on the Si(100) substrate and also shows the growth of MOF crystallites along the {110} direction. Bottom images show the growth of MOF crystallites at the defective site/point of ZnO thin film.

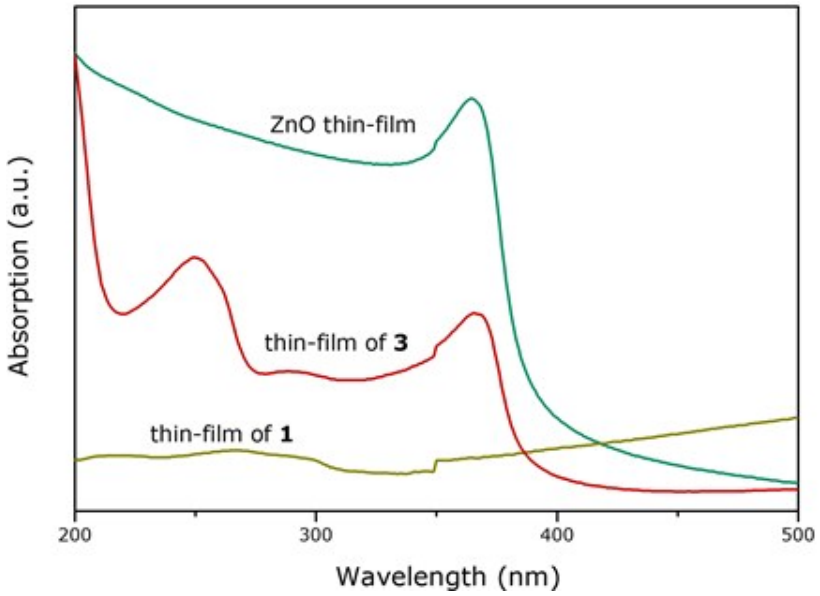

Figure S19 | UV-Vis absorption spectra of a ZnO thin film (30 nm thickness), thin films of **3** and **1**. The step at 350 nm is due to change in the detector during the measurement.

6. Single crystal analysis and structure details

Synthesis of $(DMA)_2[Zn_3(bdc)_4](H_2O)_{1.4}$(solv) single crystals:[4] A mixture of $Zn(NO_3)_2 \cdot 6H_2O$ (0.291 g, 1 mmol), H_2bdc (0.324 g, 2 mmol) in 10 mL of DMF were sealed in Teflon-lined autoclave and heated under autogenous pressure to 120 °C for 72 hrs. After the mixture was cooled to room temperature at a rate of 5 °C/h, colourless crystals of the compound were collected, washed with ethanol, and dried at room temperature(yield = 77 %).

Elemental analysis has been performed on the compound which has been dried overnight under vacuum.
Elem. Anal. ($(DMA)_2[Zn_3(bdc)_4]$; $C_{36}H_{32}N_2O_{16}Zn_3$):
Calc. for C, 45.76 %; H, 3.41 %; N, 2.96 %. Found: C, 45.11 %; H, 3.98 %; N, 2.62 %.

The crystal structure was solved with Superflip[5] and refined with SHELXL[6] using the OLEX2[7] graphical interface. All non-hydrogen atoms were refined with anisotropic atomic displacement parameters (ADPs). Hydrogen atoms were added at calculated positions and refined using a riding model with isotropic ADPs.

The DMA cation located in the pores of the framework is disordered over two sites; one major site with 70% occupancy and one minor site with 30% occupancy. Several bond length, bond angle and rigid unit restraints have been used for the refinement of the DMA cation (see CCDC 1493035 for details). A water molecule with 70% occupancy, which is hydrogen-bonding to the major component of the DMA cation, could be located in the electron density map and was included in the structural model.

The compound contains large solvent accessible voids, which are occupied by highly disordered solvent molecules. Modeling of these disordered solvents (either DMF or water) was unsuccessful. Hence, the diffuse electron density of these solvent molecules was accounted for with the *Solvent Mask* routine as implemented in Olex2. Two voids of 1128.0 $Å^3$ were found,

which contain 304.3 e^- each. This roughly corresponds to about 7 DMF molecules (40 e^- each) and 2 water molecules (10 e^- each) per void of the framework.

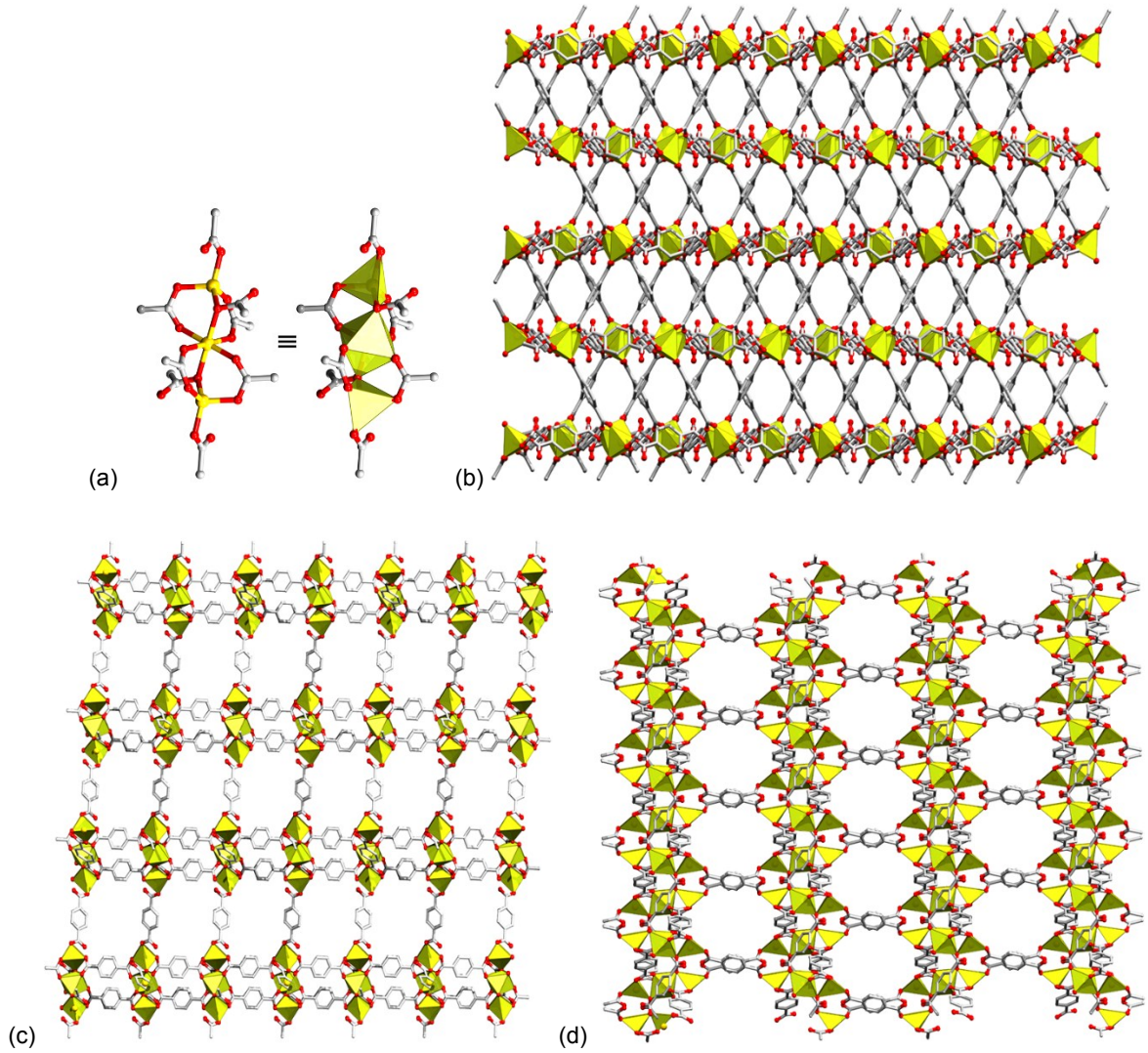

Figure S20 | The coordination geometry of Zn-metal node and its view through polyhedron view (**a**). Crystal structure of **1** along crystallographic *a*-axis (**b**), *b*-axis (**c**) and *c*-axis (**d**). The solvent, cations molecules and H-atoms were deleted for clarity.

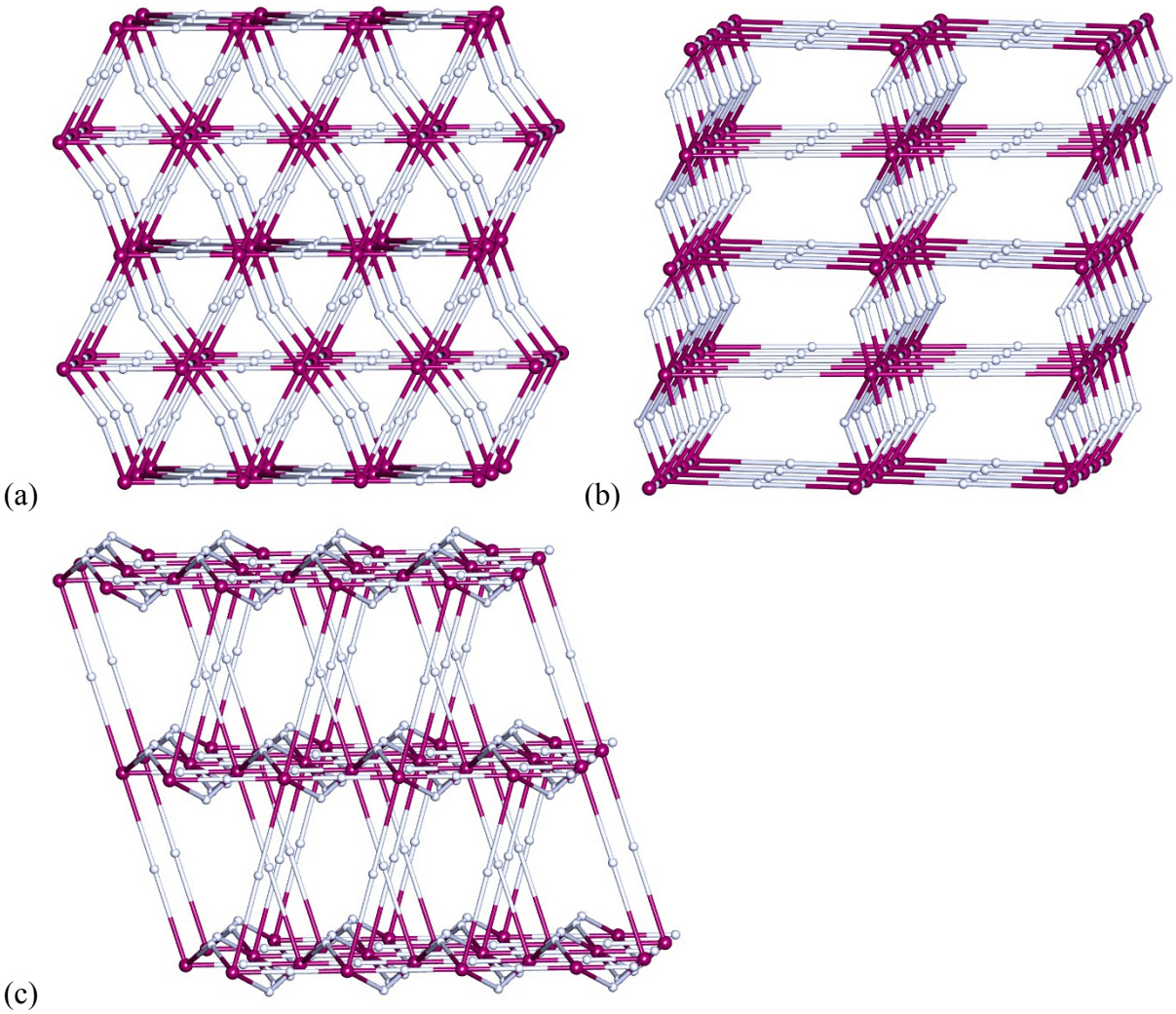

Figure S21 | Connectivity analysis in **1**, where Zn-node is considered as 8 connecting vertex (dark pink coloured ball) and bdc as a bi-connecting linker (ash coloured ball).[8]

Table S1. Crystal data and structure refinement for $(DMA)_2[Zn_3(bdc)_4](H_2O)_{1.4}(solv)$ (compound 1).

Empirical formula	$C_{36}H_{34.8}N_2O_{17.4}Zn_3$
CCDC No.	1493035
Formula weight	969.97
Temperature/K	112(3)
Crystal system	monoclinic
Space group	*C*2/*c*
a/Å	33.1191(7)
b/Å	9.72325(14)
c/Å	18.2372(3)
α/°	90
β/°	94.9516(18)
γ/°	90
Volume/Å^3	5850.94(18)
Z	4
ρ_{calc}g/cm^3	1.101
μ/mm^{-1}	1.898
F(000)	1976.0
Crystal size/mm^3	0.1918 × 0.1861 × 0.0844
Radiation	CuKα (λ = 1.54184)
2Θ range for data collection/°	9.482 to 153.634
Index ranges	$-41 \leq h \leq 41$, $-12 \leq k \leq 12$, $-21 \leq l \leq 22$
Reflections collected	63898
Independent reflections	6107 [R_{int} = 0.0709, R_{sigma} = 0.0224]
Data/restraints/parameters	6107/35/302
Goodness-of-fit on F^2	1.087
Final R indexes [I>=2σ (I)]	R_1 = 0.0402, wR_2 = 0.1155
Final R indexes [all data]	R_1 = 0.0412, wR_2 = 0.1166
Largest diff. peak/hole / e Å^{-3}	1.02/-0.93

Table S2. Fractional Atomic Coordinates (×10^4) and Equivalent Isotropic Displacement Parameters (Å^2×10^3) for 1. U_{eq} is defined as 1/3 of of the trace of the orthogonalised U_{IJ} tensor.

Atom	*x*	*y*	*z*	U(eq)
Zn1	6527.4(2)	2003.5(2)	4795.2(2)	22.62(10)
Zn2	7500	2500	5000	19.64(10)
O1	6595.3(4)	3217.1(14)	3958.9(8)	29.8(3)
O2	7272.9(4)	3078.7(13)	3969.2(7)	26.4(3)
O3	7025.5(4)	907.1(12)	5038.7(7)	25.6(3)
O4	6755.8(5)	-172.2(15)	4038.4(10)	43.9(4)
O5	5959.9(4)	1493.7(17)	4572.8(9)	39.9(3)
O6	6097.6(5)	154(2)	5546.7(10)	53.5(5)
O7	7155.1(4)	6129.8(12)	519.3(7)	25.8(3)
O8	6528.6(4)	6860.7(14)	693.6(8)	30.7(3)
C1	6930.5(5)	3426.1(18)	3689.5(10)	25.2(3)
C2	6908.5(6)	4152.8(19)	2963.7(10)	27.4(4)
C3	6541.6(6)	4670(2)	2650.4(12)	35.2(4)
C4	6521.6(6)	5320(2)	1976.4(11)	34.6(4)
C5	6870.4(6)	5463.5(19)	1604.3(10)	27.5(4)
C6	7237.0(6)	4940(2)	1912.5(11)	29.8(4)
C7	7256.5(6)	4294(2)	2589.0(11)	30.6(4)
C8	6852.2(5)	6206.0(18)	882.3(10)	25.2(3)
C9	6999.1(6)	-146.7(18)	4593.0(11)	28.9(4)
C10	7264.2(6)	-1354.2(17)	4804.0(11)	27.0(4)
C11	7496.7(6)	-1380.0(18)	5474.1(11)	28.4(4)
C12	7267.2(6)	-2478.2(18)	4327.4(12)	30.6(4)
C13	5854.5(7)	663(3)	5060.5(13)	42.7(5)
C14	5411.9(7)	311(3)	5021.3(15)	48.6(6)
C15	5275.6(8)	-649(4)	5507.3(18)	63.7(8)
C16	5138.0(8)	955(4)	4519.0(17)	63.5(8)
O1W	5839.5(17)	1443(11)	2936(3)	163(3)
N1A	6355(2)	310(6)	1998(4)	57.3(12)
N1B	6262(5)	161(17)	2052(12)	72(4)
C1A	6711.4(13)	1087(5)	1917(3)	70.8(12)
C1B	6095(4)	1010(14)	2578(8)	81(3)
C2A	6407(3)	-1136(6)	2273(5)	86(2)
C2B	6541(7)	-958(19)	2254(16)	101(7)

Table S3. Anisotropic Displacement Parameters ($Å^2 \times 10^3$) for 1. The Anisotropic displacement factor exponent takes the form: $-2\pi^2[h^2a^{*2}U_{11}+2hka^*b^*U_{12}+\ldots]$.

Atom	U_{11}	U_{22}	U_{33}	U_{23}	U_{13}	U_{12}
Zn1	22.79(15)	21.04(15)	24.51(15)	0.15(8)	4.87(10)	-3.93(8)
Zn2	21.85(17)	16.04(18)	21.58(18)	-0.92(11)	4.98(12)	-1.07(11)
O1	27.8(6)	34.3(6)	28.0(7)	7.0(5)	6.3(5)	-3.0(5)
O2	28.8(6)	26.7(6)	24.0(6)	2.2(5)	4.3(5)	-1.8(5)
O3	26.9(6)	16.9(5)	33.9(6)	-1.9(5)	8.5(5)	-3.1(5)
O4	50.8(9)	24.4(7)	53.0(9)	-6.5(6)	-15.4(7)	3.3(6)
O5	30.8(7)	46.8(9)	42.7(8)	-1.2(7)	6.1(6)	-14.7(6)
O6	33.4(8)	68.0(12)	57.7(11)	12.5(9)	-3.5(7)	-15.2(8)
O7	29.8(6)	19.6(5)	29.0(6)	3.8(5)	9.1(5)	0.8(5)
O8	28.2(7)	33.8(7)	30.9(7)	8.5(5)	7.9(5)	4.6(5)
C1	28.3(8)	21.5(8)	25.7(8)	-0.2(7)	2.6(7)	-1.8(6)
C2	27.8(8)	28.1(8)	26.7(9)	4.4(7)	5.1(7)	-3.4(7)
C3	27.2(9)	43.9(11)	35.4(10)	11.6(9)	8.2(8)	1.5(8)
C4	25.8(9)	45.3(11)	33.4(10)	13.4(9)	6.0(7)	3.3(8)
C5	29.1(9)	25.4(8)	28.5(9)	3.2(7)	6.0(7)	-0.8(7)
C6	26.6(8)	33.8(9)	30.1(9)	5.8(7)	8.4(7)	0.4(7)
C7	25.6(8)	34.7(9)	31.7(9)	6.7(8)	4.3(7)	2.4(7)
C8	26.0(8)	21.9(7)	28.5(9)	2.3(7)	7.4(7)	-2.9(6)
C9	30.9(9)	19.2(8)	36.4(10)	-1.8(7)	2.6(7)	-3.8(7)
C10	30.7(9)	16.0(7)	35.0(10)	-1.0(7)	6.6(7)	-3.5(6)
C11	36.2(9)	16.8(7)	32.5(10)	-3.5(6)	4.6(8)	-2.7(7)
C12	37.6(10)	21.5(9)	32.3(10)	-2.8(7)	0.5(8)	-2.0(7)
C13	33.2(10)	48.1(12)	46.4(12)	1.2(10)	1.3(9)	-14.4(9)
C14	32.5(10)	58.0(15)	54.6(14)	10.7(12)	-0.2(9)	-16.8(10)
C15	36.4(12)	81(2)	71.1(18)	34.0(16)	-8.7(11)	-21.2(13)
C16	41.2(13)	79(2)	68.6(18)	31.6(16)	-3.0(12)	-25.6(13)
O1W	101(4)	312(10)	73(3)	-80(5)	-5(3)	37(5)
N1A	54(3)	66(2)	50(2)	-17.0(17)	-2(2)	1.4(17)
N1B	58(6)	84(6)	71(6)	-24(5)	-12(5)	6(5)
C1A	52(2)	65(2)	93(3)	-21(2)	-11(2)	-2.7(18)
C1B	67(6)	82(7)	93(7)	-22(6)	9(6)	7(5)
C2A	120(6)	65(2)	68(4)	-12(2)	-13(4)	-5(3)
C2B	95(9)	99(8)	106(10)	-17(7)	-8(7)	31(7)

Table S4. Bond Lengths for 1.

Atom	Atom	Length/Å	Atom	Atom	Length/Å
Zn1	O1	1.9567(13)	C2	C3	1.391(3)
Zn1	O3	1.9823(13)	C2	C7	1.397(3)
Zn1	O5	1.9521(14)	C3	C4	1.379(3)
Zn1	O8[1]	1.9757(14)	C4	C5	1.396(3)
Zn2	O2	2.0427(13)	C5	C6	1.390(3)
Zn2	O2[2]	2.0427(13)	C5	C8	1.498(2)
Zn2	O3	2.2118(12)	C6	C7	1.381(3)
Zn2	O3[2]	2.2117(12)	C9	C10	1.496(2)
Zn2	O7[1]	2.0406(12)	C10	C11	1.387(3)
Zn2	O7[3]	2.0406(12)	C10	C12	1.397(3)
O1	C1	1.269(2)	C11	C12[4]	1.388(3)
O2	C1	1.249(2)	C13	C14	1.501(3)
O3	C9	1.306(2)	C14	C15	1.389(3)
O4	C9	1.238(3)	C14	C16	1.382(4)
O5	C13	1.272(3)	C15	C16[5]	1.398(3)
O6	C13	1.248(3)	N1A	C1A	1.420(8)
O7	C8	1.251(2)	N1A	C2A	1.498(8)
O8	C8	1.268(2)	N1B	C1B	1.413(17)
C1	C2	1.497(2)	N1B	C2B	1.454(15)

[1]+X,1-Y,1/2+Z; [2]3/2-X,1/2-Y,1-Z; [3]3/2-X,-1/2+Y,1/2-Z; [4]3/2-X,-1/2-Y,1-Z; [5]1-X,-Y,1-Z

Table S5. Bond Angles for 1.

Atom	Atom	Atom	Angle/°	Atom	Atom	Atom	Angle/°
O1	Zn1	O3	110.45(5)	C3	C2	C1	120.53(16)
O1	Zn1	O8[1]	108.49(6)	C3	C2	C7	119.46(17)
O5	Zn1	O1	99.47(6)	C7	C2	C1	120.00(17)
O5	Zn1	O3	132.67(6)	C4	C3	C2	120.32(18)
O5	Zn1	O8[1]	104.32(6)	C3	C4	C5	120.06(19)
O8[1]	Zn1	O3	99.94(6)	C4	C5	C8	120.20(17)
O2	Zn2	O2[2]	180.0	C6	C5	C4	119.83(17)
O2[2]	Zn2	O3[2]	90.92(5)	C6	C5	C8	119.96(16)
O2	Zn2	O3[2]	89.08(5)	C7	C6	C5	119.99(17)
O2[2]	Zn2	O3	89.08(5)	C6	C7	C2	120.33(18)
O2	Zn2	O3	90.92(5)	O7	C8	O8	125.71(17)
O3[2]	Zn2	O3	180.0	O7	C8	C5	117.61(16)
O7[1]	Zn2	O2	94.06(5)	O8	C8	C5	116.69(15)
O7[1]	Zn2	O2[2]	85.94(5)	O3	C9	C10	116.69(17)
O7[3]	Zn2	O2	85.94(5)	O4	C9	O3	121.88(18)
O7[3]	Zn2	O2[2]	94.06(5)	O4	C9	C10	121.36(17)
O7[1]	Zn2	O3[2]	89.16(5)	C11	C10	C9	120.62(17)
O7[3]	Zn2	O3	89.16(5)	C11	C10	C12	120.05(18)
O7[1]	Zn2	O3	90.84(5)	C12	C10	C9	119.31(18)
O7[3]	Zn2	O3[2]	90.84(5)	C10	C11	C12[6]	120.10(17)
O7[1]	Zn2	O7[3]	180.00(6)	C11[6]	C12	C10	119.85(19)
C1	O1	Zn1	124.19(12)	O5	C13	C14	115.9(2)
C1	O2	Zn2	134.39(12)	O6	C13	O5	123.4(2)
Zn1	O3	Zn2	101.31(5)	O6	C13	C14	120.7(2)
C9	O3	Zn1	105.82(12)	C15	C14	C13	119.5(2)
C9	O3	Zn2	122.63(11)	C16	C14	C13	120.7(2)
C13	O5	Zn1	109.46(14)	C16	C14	C15	119.8(2)
C8	O7	Zn2[4]	135.53(12)	C14	C15	C16[7]	119.5(3)
C8	O8	Zn1[5]	116.54(12)	C14	C16	C15[7]	120.8(2)
O1	C1	C2	116.15(16)	C1A	N1A	C2A	117.4(6)
O2	C1	O1	126.33(17)	C1B	N1B	C2B	122.9(16)
O2	C1	C2	117.52(16)				

[1]+X,1-Y,1/2+Z; [2]3/2-X,1/2-Y,1-Z; [3]3/2-X,-1/2+Y,1/2-Z; [4]3/2-X,1/2+Y,1/2-Z; [5]+X,1-Y,-1/2+Z; [6]3/2-X,-1/2-Y,1-Z; [7]1-X,-Y,1-Z

Table S6. Torsion Angles for 1.

A	B	C	D	Angle/°	A	B	C	D	Angle/°
Zn1	O1	C1	O2	-11.6(3)	O6	C13	C14	C15	-3.5(4)
Zn1	O1	C1	C2	168.01(12)	O6	C13	C14	C16	175.0(3)
Zn1	O3	C9	O4	15.6(2)	C1	C2	C3	C4	-179.0(2)
Zn1	O3	C9	C10	-161.61(13)	C1	C2	C7	C6	178.73(18)
Zn1	O5	C13	O6	-7.6(3)	C2	C3	C4	C5	0.0(4)
Zn1	O5	C13	C14	172.59(18)	C3	C2	C7	C6	-0.1(3)
Zn1[1]	O8	C8	O7	-6.2(3)	C3	C4	C5	C6	0.5(3)
Zn1[1]	O8	C8	C5	173.74(12)	C3	C4	C5	C8	-178.2(2)
Zn2	O2	C1	O1	-17.2(3)	C4	C5	C6	C7	-0.8(3)
Zn2	O2	C1	C2	163.22(12)	C4	C5	C8	O7	-169.52(18)
Zn2	O3	C9	O4	-99.4(2)	C4	C5	C8	O8	10.5(3)
Zn2	O3	C9	C10	83.34(18)	C5	C6	C7	C2	0.6(3)
Zn2[2]	O7	C8	O8	48.6(3)	C6	C5	C8	O7	11.8(3)
Zn2[2]	O7	C8	C5	-131.36(15)	C6	C5	C8	O8	-168.15(18)
O1	C1	C2	C3	5.7(3)	C7	C2	C3	C4	-0.2(3)
O1	C1	C2	C7	-173.09(18)	C8	C5	C6	C7	177.92(18)
O2	C1	C2	C3	-174.64(18)	C9	C10	C11	C12[3]	178.20(18)
O2	C1	C2	C7	6.5(3)	C9	C10	C12	C11[3]	-178.23(18)
O3	C9	C10	C11	5.6(3)	C11	C10	C12	C11[3]	0.0(3)
O3	C9	C10	C12	-176.19(17)	C12	C10	C11	C12[3]	0.0(3)
O4	C9	C10	C11	-171.64(19)	C13	C14	C15	C16[4]	178.6(3)
O4	C9	C10	C12	6.6(3)	C13	C14	C16	C15[4]	-178.6(3)
O5	C13	C14	C15	176.3(3)	C15	C14	C16	C15[4]	-0.1(6)
O5	C13	C14	C16	-5.2(4)	C16	C14	C15	C16[4]	0.1(6)

[1]+X,1-Y,-1/2+Z; [2]3/2-X,1/2+Y,1/2-Z; [3]3/2-X,-1/2-Y,1-Z; [4]1-X,-Y,1-Z

Table S7. Hydrogen Atom Coordinates (Å×10^4) and Isotropic Displacement Parameters (Å^2×10^3) for 1.

Atom	*x*	*y*	*z*	U(eq)
H3	6308.73	4575.63	2896.65	42
H4	6275.64	5664.15	1769.45	42
H6	7469.06	5023.86	1663.05	36
H7	7502.66	3952.22	2796.18	37
H11	7494.38	-630.88	5790.79	34
H12	7111.44	-2461.3	3878.12	37
H15	5458.01	-1085.27	5847.35	76
H16	5229.77	1598.06	4194.62	76
H1WA	5720.81	1611.24	3321.33	244
H1WB	5687.65	1688.37	2558.33	244
H1AA	6211.21	281.92	1562.66	69
H1AB	6207.37	762.42	2304.8	69
H1BA	6388.25	716.7	1758.44	86
H1BB	6054.26	-205.46	1778.37	86
H1AC	6870.4	635.86	1572.52	106
H1AD	6866.67	1159.33	2384.94	106
H1AE	6638.09	1989.68	1739.27	106
H1BC	5950.94	1757.42	2332.59	121
H1BD	6309.22	1367.38	2913.62	121
H1BE	5912.54	480.06	2846.47	121
H2AA	6556.56	-1656.34	1939.39	128
H2AB	6146.32	-1549.64	2304.96	128
H2AC	6553.42	-1130.24	2751.43	128
H2BA	6449.19	-1779.96	1999.59	151
H2BB	6551.65	-1109.92	2775.21	151
H2BC	6806.42	-723.73	2119.41	151

Table S8. Atomic Occupancy for 1.

Atom	*Occupancy*	Atom	*Occupancy*	Atom	*Occupancy*
O1W	0.7	H1WA	0.7	H1WB	0.7
N1A	0.7	H1AA	0.7	H1AB	0.7
N1B	0.3	H1BA	0.3	H1BB	0.3
C1A	0.7	H1AC	0.7	H1AD	0.7
H1AE	0.7	C1B	0.3	H1BC	0.3
H1BD	0.3	H1BE	0.3	C2A	0.7
H2AA	0.7	H2AB	0.7	H2AC	0.7
C2B	0.3	H2BA	0.3	H2BB	0.3
H2BC	0.3				

Table S9. Solvent masks information for 1.

Number	X	Y	Z	Volume	Electron count	Content
1	0.000	0.083	-0.015	1128.0	304.3	DMF, water
2	0.500	-0.305	-0.084	1128.0	304.3	DMF, water

References

1. D. Bekermann, A. Ludwig, T. Toader, C. Maccato, D. Barreca, A. Gasparotto, C. Bock, A. D. Wieck, U. Kunze, E. Tondello, R. A. Fischer and A. Devi, *Chem. Vap. Deposition*, 2011, **17**, 155-161.
2. H. He, *Acta Crystallogr. E*, 2006, **62**, m3291-m3292.
3. H. Li, M. Eddaoudi, M. O'Keeffe and O. M. Yaghi, *Nature*, 1999, **402**, 276-279.
4. a) S. A. Sapchenko, D. N. Dybtsev, D. G. Samsonenko and V. P. Fedin, *New J. Chem.*, 2010, **34**, 2445-2450; b) Z. Jiang, Y. An, X. Zhu, C. Tian, J. Bai and Y. Li, *Z. Anorg. Allg. Chem.*, 2015, **641**, 2599-2603.
5. L. Palatinus and G. Chapuis, *J. Appl. Crystallogr.*, 2007, **40**, 786-790.
6. G. Sheldrick, *Acta Crystallogr. C*, 2015, **71**, 3-8.
7. O. V. Dolomanov, L. J. Bourhis, R. J. Gildea, J. A. K. Howard and H. Puschmann, *J. Appl. Crystallogr.*, 2009, **42**, 339-341.
8. a) V. A. Blatov, A. P. Shevchenko and D. M. Proserpio, *Cryst. Growth. Des.*, 2014, **14**, 3576-3586; b) M. Li, D. Li, M. O'Keeffe and O. M. Yaghi, *Chem. Rev.*, 2014, **114**, 1343-1370.